PRZEGLĄD ELEKTROTECHNICZNY

OPEN ACCESS

Rafał GABOR[1], Marcin KULIK[2]

ORCID: [1]0000-0001-7704-5088, [2]0000-0003-0120-3523

DOI: 10.15199/48.2025.11.5

Influence of beam material on the voltage and power responses in a nonlinear electromagnetic energy harvester

Wpływ materiału belki na odpowiedzi częstotliwościowe w nieliniowym elektromagnetycznym układzie pozyskiwania energii z drgań

[1] dr inż. Rafał Gabor, Opole University of Technology, Faculty of Electrical Engineering, Automatic Control and Informatics, ul. Prószkowska 76, 45-758 Opole, e-mail: r.gabor@po.edu.pl

[2] dr inż. Marcin Kulik, Opole University of Technology, Faculty of Electrical Engineering, Automatic Control and Informatics, ul. Prószkowska 76, 45-758 Opole, e-mail: m.kulik@po.edu.pl

Correspondence address: r.gabor@po.edu.pl

Abstract: This study investigates how the choice of beam material affects the dynamic performance of a nonlinear electromagnetic energy harvester. Four materials—carbon fiber, fiberglass, aluminum, and ABS – were analyzed by optimizing their beam cross-sections (at a fixed length) to achieve a common resonance frequency of 35 Hz. Despite identical natural frequencies, modal and dynamic simulations revealed notable differences in vibration response, voltage output, power generation, and stress distribution. Composite materials, particularly carbon fiber and fiberglass, produced higher output voltages and power, while aluminum offered a wider operational bandwidth. Stress analyses under identical displacements showed significant variation in maximum stress, driven primarily by differences in Young's modulus. The presented methodology supports material- and geometry-aware design of efficient, durable energy harvesters for use in autonomous, vibration-powered devices.

Keywords: energy harvesting, nonlinear dynamics, stress analysis, vibration energy conversion

Streszczenie: Niniejszy artykuł ukazuje, w jaki sposób wybór materiału belki wpływa na charakterystyki dynamiczne nieliniowego elektromagnetycznego układu pozyskiwania energii. Cztery materiały – włókno węglowe, włókno szklane, aluminium oraz ABS — zostały przeanalizowane poprzez optymalizację przekrojów poprzecznych belek (przy stałej długości) w celu uzyskania wspólnej częstotliwości rezonansowej wynoszącej 35 Hz. Pomimo identycznych częstotliwości własnych, symulacje modalne i dynamiczne ujawniły istotne różnice w odpowiedzi drganiowej, generowanym napięciu, wytwarzanej mocy oraz rozkładzie naprężeń. Materiały kompozytowe, w szczególności włókno węglowe i szklane, wykazały wyższe wartości napięcia wyjściowego i mocy, natomiast aluminium charakteryzowało się szerszym pasmem roboczym. Analizy naprężeń przy identycznych przemieszczeniach wykazały znaczną zmienność maksymalnych naprężeń, wynikającą głównie z różnic w module Younga. Zaprezentowana metodologia wspiera projektowanie wydajnych i trwałych układów pozyskiwania energii, uwzględniających materiał i geometrię, przeznaczonych do zastosowań w autonomicznych urządzeniach zasilanych drganiami.

Słowa kluczowe: pozyskiwanie energii, konwersja drgań, analiza naprężeń, układy nieliniowe

Introduction

With the advancement of modern technologies in manufacturing systems, complex automation setups–comprising drives, sensors, and data processing systems–are being increasingly employed [1-3]. Although such solutions enhance process flexibility and efficiency, they also contribute to a significant increase in electrical energy demand [4]. In the light of rising energy costs and the global need to reduce greenhouse gas emissions, alternative energy harvesting methods are gaining increasing attention [5-7].

One intensively developing area in response to growing energy needs is ambient energy harvesting, which enables the conversion of energy from local sources–such as vibrations, heat, airflow, or electromagnetic radiation–into electrical energy [6-8]. Due to their specific characteristics, these technologies are particularly well-suited for powering autonomous devices, such as wireless sensors and Internet of Things (IoT) components, where long-term operation without battery replacement or wired power supply is crucial [1,9-13].

Depending on the nature of the available energy sources, it becomes essential to select an appropriate energy conversion technology capable of operating efficiently under variable environmental conditions. One commonly used energy harvesting mechanism involves vibrating systems that convert mechanical energy–originating, for example, from structural, machine, or ground vibrations–into electrical energy [14-16]. These harvesters may utilize piezoelectric, electromagnetic, or electrostatic phenomena, and their core functional element is typically a vibrating beam coupled with an appropriate energy conversion system [15,17,18].

The effectiveness of such harvesters largely depends on their dynamic characteristics, particularly their ability to operate within the frequency range of environmental excitation [19,20]. Traditional linear resonant systems are efficient only within a narrow frequency band near their resonance, which limits their practical application in real-world conditions, where excitation parameters–such as amplitude and frequency–often fluctuate or are difficult to predict [19].

To overcome these limitations, there is a growing interest in harvesters utilizing nonlinear resonance phenomena. These solutions enable a broader operational bandwidth, resulting in higher energy yield [2,21]. Nonlinear systems, thanks to the presence of elements such as nonlinear springs, mechanical stoppers, or nonlinear magnetic forces, can exhibit an expanded resonance band along with phenomena such as bifurcations, hysteresis, and amplitude jumps [14,22]. This enables more efficient energy harvesting under variable excitation without the need for active tuning to the changing frequency. Such characteristics are particularly desirable in autonomous devices, where external control or adaptation of operating parameters is not feasible.

However, the effectiveness of such devices depends not only on their working principles but also on the appropriate design of structural components and the selection of suitable materials. In the case of miniature energy generators, a tailored design approach is required, in which the optimal matching of both geometry and material properties of energy-converting elements plays a critical role [23,24]. The vibrating beam, in particular, requires careful analysis, as its shape, stiffness, and stress distribution directly affect the energy efficiency and stability of the system [1,13,25]. Material properties such as Young's modulus, damping, and density determine the beam's resonance frequency and dynamic response under real operating conditions [26,27].

This study aims to analyze how the geometry and material properties of a vibrating beam influence the performance of a nonlinear electromagnetic energy harvester. A numerical model of the system was developed, maintaining a constant beam length while optimizing the cross-sectional dimensions of beams made from four different materials–carbon fiber, fiberglass, aluminum, and ABS–to achieve a uniform resonance frequency of 35 Hz. It is a value that represents a compromise between sources of vibrations of low frequency (on the order of several tens of hertz) and sources of vibrations with frequencies close to 50 Hz. By performing modal and dynamic simulations, the study evaluates how material selection affects displacement behavior, magnetic force, voltage output, and power generation under a consistent vibration acceleration level. Additionally, a comparative stress analysis under identical tip displacements was conducted to assess structural durability. Unlike previous research that focused predominantly on geometry or theoretical modeling, this work directly compares the material-dependent trade-offs in identically tuned nonlinear harvesters. The approach presented here provides a practical design framework for enhancing the efficiency and mechanical reliability of energy harvesting systems, particularly in autonomous or battery-free applications.

Nonlinear Electromagnetic Energy Harvester

This study presents an electromagnetic vibration energy harvester consisting of a flat beam, yoke with permanent magnets, two parallel-connected coils, and additional permanent magnets (Fig. 1). Under the influence of external mechanical vibrations, the flat beam bends, inducing an electric voltage in the coils, which remain stationary relative to the yoke. The considered system operates based on the principle of nonlinear mechanical resonance. This means that the frequency response of the electromotive force in the coils depends on both the resonance frequency of the flat beam and the resonance frequency of the magnetic suspension (formed by the magnets on the yoke and the additional magnets mounted on a support structure). The former frequency remains constant, while the latter depends on the displacement amplitude of the flat beam. As a result, it is possible to obtain frequency response characteristics with a broad operational bandwidth, which increases with vibration acceleration.

To determine these characteristics, a computational model was proposed based on Timoshenko beam theory [28] and analytical formulas for calculating the integral parameters of the magnetic circuit [23,29]

$$M\frac{d^2z}{dt^2} + D\frac{dz}{dt} + Kz = b(ma_{vib} - F_{mag} - F_e - mg) \quad (1)$$

where:
M, D and K – the global mass, damping, and stiffness matrices,
z – the vector containing the displacements and velocities of the beam nodes as well as the current flowing through the coils,
b – the vector assigning external forces to the corresponding variables at the beam's tip node.
The parameters m, a_{vib}, F_{mag}, F_e, g and t represent, respectively, the mass of the yoke with permanent magnets, vibration acceleration, magnetic force (Fig. 2), electromotive force, gravitational acceleration, and time. This equation, coupled with the electrical circuit equation, is used to determine the frequency response characteristics of the analyzed system

$$L_c\frac{di(t)}{dt} = \frac{\partial\lambda(\zeta)}{\partial\zeta}\frac{d\zeta(t)}{dt} - (R_L + R_c)i \quad (2)$$

where L_c, R_c, i, λ, ζ and R_L denote, respectively, the inductance and resistance of the parallel-connected coils, the current flowing in the electrical circuit, the magnetic flux linkage (its derivative with respect to displacement is shown in Fig. 3), the displacement of the beam's tip node, and the load resistance. The system is designed so that the resonance frequency of the flat beam is reached at higher vibration acceleration levels. To achieve this, the additional permanent magnets must soften the beam's stiffness; thus, their polarity is oriented to attract the magnets mounted on the yoke. The resonance frequency of the beam can be determined from the following equation:

$$f_r = \frac{1}{2\pi}\sqrt{\frac{k}{m}} \quad (3)$$

where k is a beam stiffness.

Geometry optimization

In the design of mechanical vibration energy harvesting systems, tuning the dynamic characteristics to the operating conditions is of critical importance. One of the fundamental tools used to assess system behavior under dynamic loading is modal analysis, which allows for the determination of the natural vibration frequencies and their corresponding mode shapes. In engineering practice, the most commonly used information is the first natural frequency, which determines the maximum energy conversion efficiency in resonant systems. Proper tuning of the system to the desired resonance frequency requires precise adjustment of the geometric parameters and consideration of the material properties of the components.

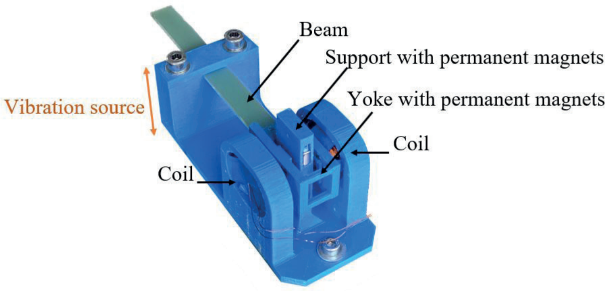

Fig. 1. System for converting mechanical energy into electrical energy using a mini-generator based on electromagnetic induction and non-linear mechanical resonance

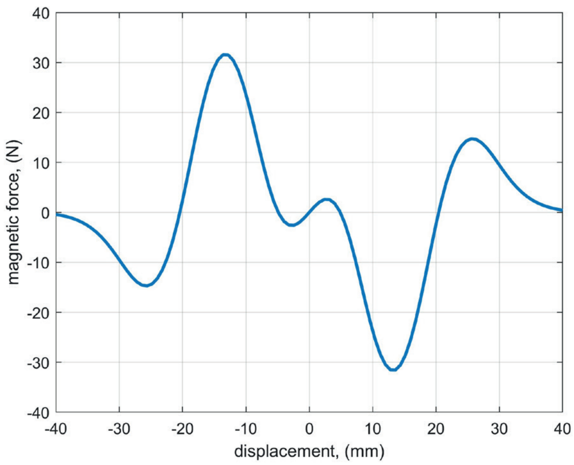

Fig. 2. Magnetic force as a function of the beam tip displacement

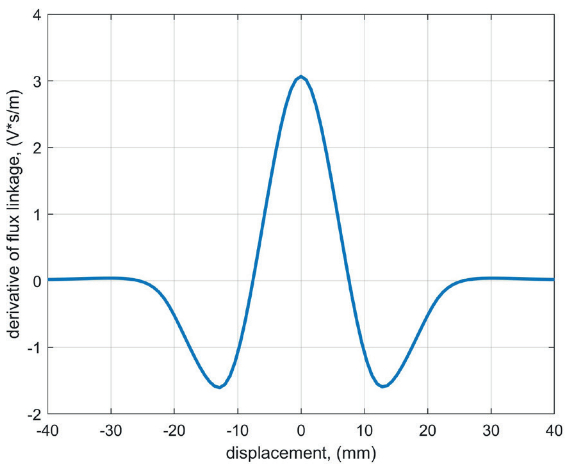

Fig. 3. Derivative of flux linkage depending on the beam tip displacement

This chapter presents the process of optimizing the geometric dimensions of the beam under the assumption of constant length, in order to obtain a first resonance frequency of approximately 35 Hz (Fig. 4). The calculations were performed for four different materials using modal analysis. Table 1 summarizes the basic material properties of the selected materials, while Table 2 compares the optimized cross-sectional dimensions of the beam for each case.

Table 1. Materials parameters

Parameters	Fiberglass	Carbon fiber	Aluminium	ABS
Density [kg/m³]	2075	1580	2700	1070
Young Modulus [GPa]	12.28	130	70	2.28
Poission Ratio [-]	0.12	0.3	0.33	0.38

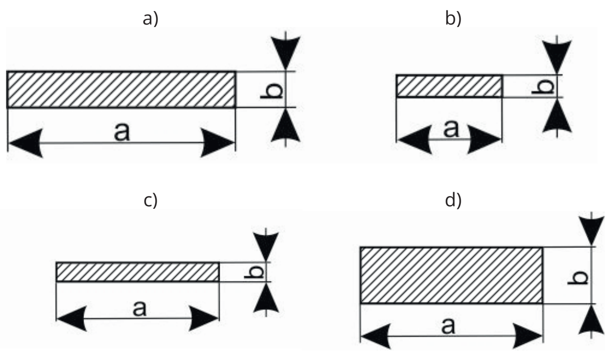

Fig. 4. Cross-sections of optimized beams made of the following materials: Fiberglass (a), Carbon fiber (b), Aluminium (c), ABS (d)

Table 2. Cross-sectional dimensions of the vibrating beam

Dimensions	Fiberglass	Carbon fiber	Aluminium	ABS
width *a* [mm]	16	7.4	13.1	14.7
thickness *b* [mm]	2.5	1.5	1.5	4.5
length *l* [mm]	75	75	75	75

In the presented case, the mechanical system of the energy harvester's beam is analyzed under free vibration conditions–that is, without considering external forces or damping. For such a system, the classical equation of motion reduces to the so-called eigenvalue problem, which forms the basis of modal analysis [30]:

$$(\boldsymbol{K} - \omega_{0i}^2 \boldsymbol{M})\boldsymbol{\Phi}_{0i} = 0 \tag{4}$$

This equation has non-trivial solutions only when the determinant of the system matrix equals zero, which leads to an eigenvalue problem. Solving this problem allows for the determination of discrete eigenvalues ω^2_{0i}, and consequently, the corresponding natural frequencies ω_{0i} . Each of these frequencies is associated with a unique mode shape Φ_{0i}, which can be obtained from equation (4) for the given value of ω_{0i}.

For each material, the optimized cross-sectional dimensions were determined, followed by the calculation of the corresponding first vibration mode and its associated natural frequency (Fig. 5.). The finite element mesh size was selected so that further refinement did not lead to significant changes in the calculated natural frequency. The obtained results showed that, despite significant differences in material properties, an appropriate selection of geometry allows for achieving similar mode shapes. This confirms the effectiveness of the optimization approach in designing resonant vibration energy harvesters tailored to specific operating conditions.

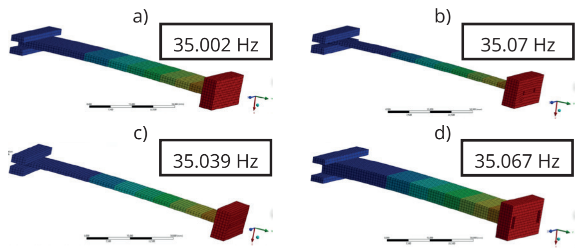

Fig.5. First vibration mode shapes of the beam for different materials: Fiberglass (a), Carbon fiber (b), Aluminium (c), ABS (d)

Frequency Response Analysis

With the geometric parameters of the considered beams established, frequency response calculations were performed using the model defined by equations (1)–(2). These responses are obtained for an acceleration signal with a constant root mean square (RMS) value and linearly varying frequency. Figure 6 shows the displacement envelopes as a function of vibration frequency (ranging from 10 to 45 Hz). As can be observed, despite the identical resonance frequencies of the analyzed beams, their displacement characteristics differ. The higher the vibration acceleration, the more pronounced these differences become. The most similar responses were obtained for the fiberglass and carbon fiber beams, while the ABS beam shows a slightly larger deviation. The aluminum beam, however, exhibits the most distinct displacement behavior compared to the others.

Figure 7 illustrates the frequency characteristics of the voltage amplitude generated by the energy harvester with a load resistance of R_L = 100Ω, evaluated across different beam materials under identical operating conditions. As vibration acceleration increases, the aluminum beam demonstrates a broader operational frequency band, indicating its ability to maintain a response over a wider range of excitation frequencies. However, this broader bandwidth comes at the cost of lower voltage output compared to the other materials. The voltage gap between the aluminum beam and the higher-performing composite beams–particularly carbon fiber and fiberglass–widens with increasing acceleration, reaching approximately 0.5 V at 7.5 m/s². This trade-off highlights the aluminum beam's limited voltage efficiency despite its extended frequency response.

Figure 8 shows the output power characteristics obtained across a resistive load of 100 Ω. The observed

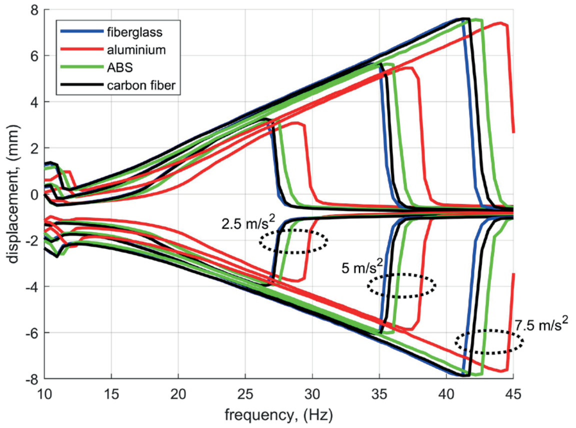

Fig. 6. Frequency characteristics of envelope of beam tip displacement for different beam materials and acceleration of vibration – frequency sweep from 10 to 45 Hz

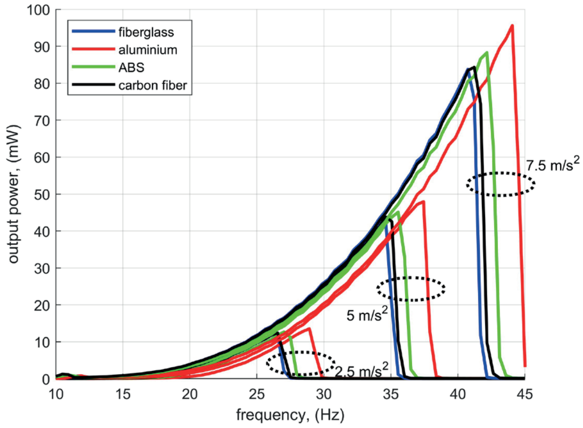

Fig. 8. Frequency characteristics of output power for different beam materials and acceleration of vibration – frequency sweep from 10 to 45 Hz

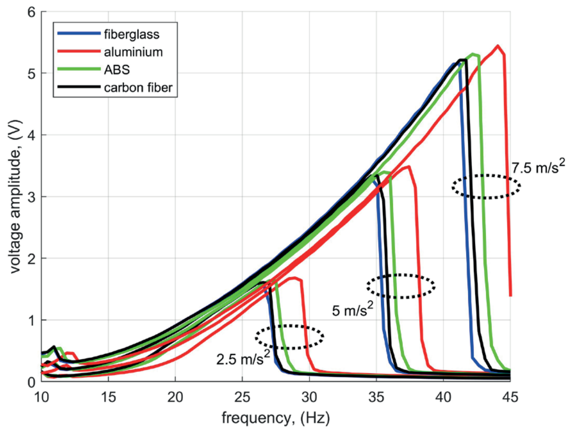

Fig. 7. Frequency characteristics of voltage amplitude for different beam materials and acceleration of vibration – frequency sweep from 10 to 45 Hz

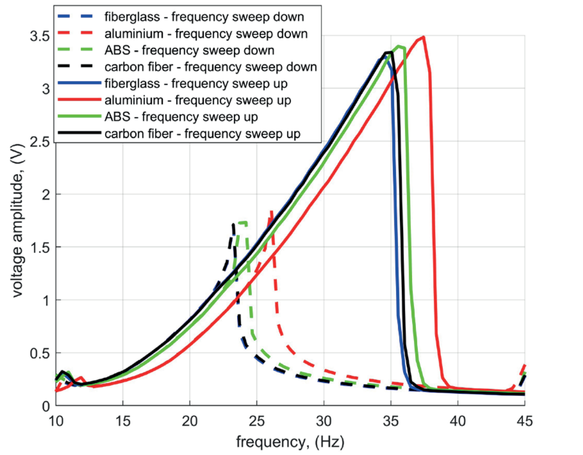

Fig. 9. Frequency characteristics of voltage amplitude for different beam materials – rms value of vibration acceleration is equat to 5 m/s²

trends are fully consistent with those presented in Figure 7 – given the quadratic relationship between voltage and power, it is possible to predict the output power values based on the voltage amplitude.

Figure 9 presents a comparison of voltage characteristics depending on the direction of frequency sweep (increasing and decreasing), at a constant vibration acceleration of 5 m/s². Differences in the position and shape of the resonance peak can be observed depending on the sweep direction, indicating the presence of frequency hysteresis typical for systems with nonlinear stiffness.

Mechanical analysis

The mechanical analysis of the energy harvester system was conducted for beams made of different materials subjected to excitations with varying acceleration levels, as shown in Figure 6. Particular attention was given to two key mechanical parameters: the maximum displacement at the beam tip and the corresponding maximum stress occurring in critical cross-sectional regions. The analysis considered three vibration acceleration values: 2.5 m/s², 5 m/s², and 7.5 m/s². The simulation was conducted using static analysis, with one end fixed and the other displaced to reproduce the maximum displacement corresponding to the vibration acceleration. The results are summarized in Table 3.

Despite similar deflections, significant differences in stress values are observed, which result directly from the mechanical properties of the applied materials–primarily from Young's modulus.

To enable a direct comparison of stress distributions arising solely from material and geometric differences–independent of acceleration–an additional numerical analysis was conducted, in which each beam was subjected to an identical yoke displacement of 5 mm. This approach allowed for visualization of the maximum stress values and their locations (Fig. 10).

Regardless of the material, the locations of maximum stress remain similar–they are concentrated

Table 3. Summary of stress values for different yoke displacements

Acceleration	Beam materials	Max displacement [mm]	Max stress [MPa]	Typical Fatigue Limit [MPa]
2.5 m/s²	Fiberglass	3.14	26.64	~100-150
	Carbon fiber	3.24	166.55	~400-800
	Aluminium	3.07	90.185	~97
	ABS	3.2	12.3	~15-25
5 m/s²	Fiberglass	5.63	47.76	~100-150
	Carbon fiber	5.66	290.95	~400-800
	Aluminium	5.45	160.1	~97
	ABS	5.62	21.6	~15-25
7.5 m/s²	Fiberglass	7.55	64.05	~100-150
	Carbon fiber	7.58	389.64	~400-800
	Aluminium	7.4	217.38	~97
	ABS	7.55	29.02	~15-25

in the clamping zone of the beam, which is a typical characteristic of cantilever systems operating under bending conditions. To evaluate the fatigue durability of the beams under dynamic excitation, the maximum stress values obtained at the highest excitation level (acceleration of 7.5 m/s²) were compared with the typical fatigue limits for each material, as summarized in Table 3. These reference values were adopted based on data available in the literature and experimental studies [31-36] The analysis shows that stresses in the fiberglass beam remain well below its fatigue threshold, indicating safe long-term operation. In the case of carbon fiber, the stress level approaches the lower bound of the fatigue range, but with proper fiber orientation and laminate quality, the material can still be considered safe. In contrast, the stress levels in the aluminum and ABS beams reach or exceed commonly accepted fatigue limits, indicating a risk of fatigue failure under prolonged dynamic loading.

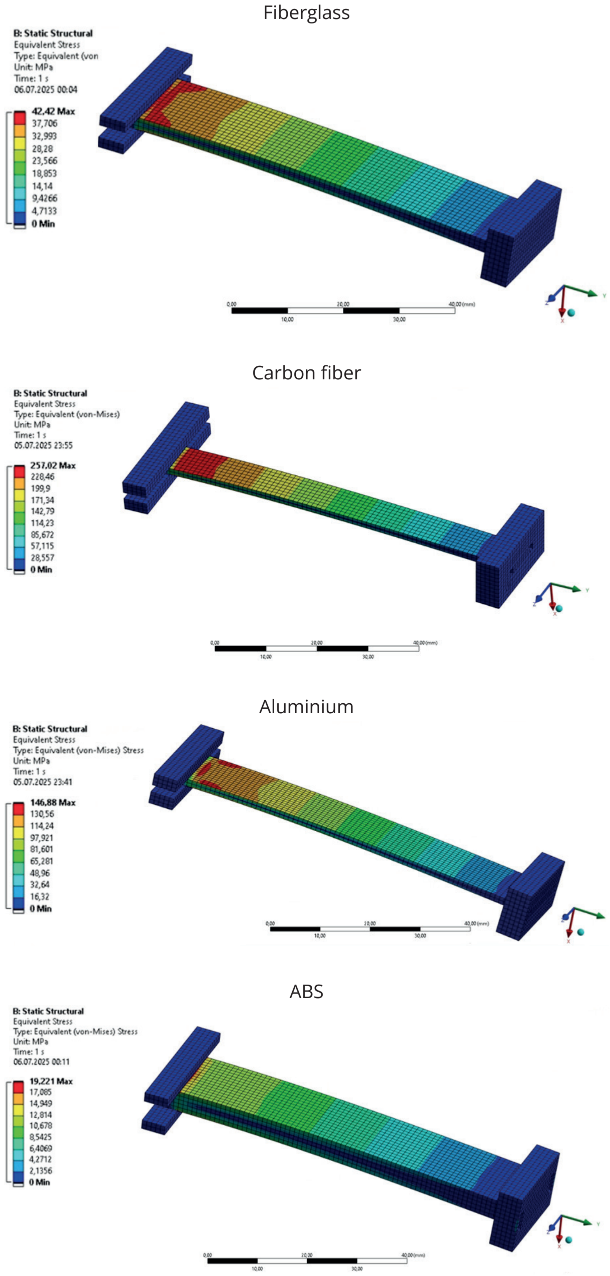

Fig. 10. Stress values for a yoke displacement of 5 mm

The stress analysis revealed that, for identical beam tip displacements, there were substantial differences in the maximum stress values, primarily determined by the Young's modulus of the material. The highest stresses were recorded in carbon fiber beams, while the lowest were observed in ABS beams, which was attributed to the varying thicknesses of the beam cross-sections. It has been shown that, taking the fatigue limit into account, only the fiberglass beam has an adequate safety margin under the considered operating conditions.

In the next stage of research, the authors will focus on fatigue analysis of the considered beams.

Conclusions

Based on the conducted study, it was found that the dynamic characteristics of the energy harvester system–including displacements, voltages, and output power–differed significantly depending on the material properties. In particular, systems with beams made of composite materials such as carbon fiber and fiberglass exhibited higher voltages and power outputs compared to beams made of aluminum or ABS, especially at lower acceleration levels. However, the aluminum beam demonstrated a broader frequency bandwidth within which relatively high voltage was generated.

Received: 30.09.2025, **Accepted:** 24.10.2025, **Published:** 24.11.2025

REFERENCES

[1] Norenberg JP., Luo R., Lopes VG., Peterson JVLL., Cunha A., Nonlinear dynamics of asymmetric bistable energy harvesters, International Journal of Mechanical Sciences vol. 257, Elsevier Ltd; (2023), DOI: 10.1016/j.ijmecsci.2023.108542

[2] Won SS., Kawahara M., Glinsek S., Lee J., Kim Y., Jeong CK., et al., Flexible vibrational energy harvesting devices using strain-engineered perovskite piezoelectric thin films, Nano Energy vol. 55, 182–92, Elsevier Ltd; (2019), DOI: 10.1016/J.NANOEN.2018.10.068.

[3] Xu X., Lu Y., Vogel-Heuser B., Wang L., Industry 4.0 and Industry 5.0 – Inception, conception and perception, Journal of Manufacturing Systems vol. 61, 530–5, Elsevier; (2021), DOI: 10.1016/J.JMSY.2021.10.006.

[4] Rojek I., Dostatni E., Pawłowski L., W. Egrzyn-Wolska KM., Sustainability in production in the aspect of Industry 4.0, Bulletin Of The Polish Academy Of Sciences Technical Sciences vol. 70, no. 6, 143832, (2022), DOI: 10.24425/bpasts.2022.143832.

[5] Sezer N., Koç M., A comprehensive review on the state-of-the-art of piezoelectric energy harvesting, Nano Energy vol. 80, Elsevier Ltd; (2021), DOI: 10.1016/J.NANOEN.2020.105567.

[6] Zuo L., Tang X., Large-scale vibration energy harvesting, Journal of Intelligent Material Systems and Structures vol. 24, no. 11, 1405–30, (2013), DOI: 10.1177/1045389X13486707.

[7] Mitcheson PD., Yeatman EM., Rao GK., Holmes AS., Green TC., Energy harvesting from human and machine motion for wireless electronic devices, Proceedings of the IEEE vol. 96, no. 9, 1457–86, Institute of Electrical and Electronics Engineers Inc.; (2008), DOI: 10.1109/JPROC.2008.927494.

[8] Jang J., Hwang GT., Min Y., Kim JW., Ahn CW., Choi JJ., et al., Fatigue study and durability improvement of piezoelectric single crystal macro-fiber composite energy harvester, Journal of the Korean Ceramic Society vol. 57, no. 6, 645–50, Springer; (2020), DOI: 10.1007/S43207-020-00062-9.

[9] Nord JH., Koohang A., Paliszkiewicz J., The Internet of Things: Review and theoretical framework, Expert systems with applications vol. 133, 97–108, Elsevier Ltd; (2019), DOI: 10.1016/J.ESWA.2019.05.014.

[10] Abdelkareem MAA., Xu L., Ali MKA., Elagouz A., Mi J., Guo S., et al., Vibration energy harvesting in automotive suspension system: A detailed review, Applied Energy vol. 229, 672–99, Elsevier Ltd; (2018), DOI: 10.1016/J.APENERGY.2018.08.030.

[11] Phillips JD., Energy Harvesting in Nanosystems: Powering the Next Generation of the Internet of Things, Frontiers in Nanotechnology vol. 3, Frontiers Media S.A.; (2021), DOI: 10.3389/FNANO.2021.633931/FULL.

[12] Kazemi S., Nili-Ahmadabadi M., Tavakoli MR., Tikani R., Energy harvesting from longitudinal and transverse motions of sea waves particles using a new waterproof piezoelectric waves energy harvester, Renewable Energy vol. 179, 528–36, Elsevier Ltd; (2021), DOI: 10.1016/J.RENENE.2021.07.042.

[13] Challa VR., Prasad MG., Shi Y., Fisher FT., A vibration energy harvesting device with bidirectional resonance frequency tunability, Smart Materials and Structures vol. 17, no. 1, (2008), DOI: 10.1088/0964-1726/17/01/015035.

[14] Rosso M., Ardito R., A Review of Nonlinear Mechanisms for Frequency Up-Conversion in Energy Harvesting, Actuators 2023, Vol. 12, Page 456 vol. 12, no. 12, 456, Multidisciplinary Digital Publishing Institute; (2023), DOI: 10.3390/ACT12120456.

[15] Farhan M., Muthalif AGA., Ali MSM., Innovative approaches to optimize vibration energy harvesting (VEH): A comprehensive review, Energy Reports vol. 12, 5194–219, Elsevier Ltd; (2024), DOI: 10.1016/J.EGYR.2024.11.006.

[16] Jagiela M., Kulik M., Action of torsion and axial moment in a new nonlinear cantilever-type vibration energy harvester, International Journal of Applied Electromagnetics and Mechanics vol. 57, no. 51, S135–42, IOS Press; (2018), DOI: 10.3233/JAE-182304.

[17] Ahmad MM., Khan FU., Review of vibration-based electromagnetic–piezoelectric hybrid energy harvesters, International Journal of Energy Research vol. 45, no. 4, 5058–97, John Wiley and Sons Ltd; (2021), DOI: 10.1002/ER.6253;PAGE:STRING:ARTICLE/CHAPTER.

[18] Xiao Y., Han Q., Wu N., Piezoelectric energy harvesting: a review of energy sources, structures, and working mechanisms in high-frequency excitations and operations, Smart Materials and Structures vol. 34, no. 2, Institute of Physics; (2025), DOI: 10.1088/1361-665X/ADADCC.

[19] Zhang X., Zhu F., Chen L., Chen X., Guo Y., Xu H., Dynamic Characteristics and Experimental Research of Linear-Arch Bi-Stable Piezoelectric Energy Harvester, Micromachines vol. 13, no. 5, 814, MDPI; (2022), DOI: 10.3390/MI13050814.

[20] Wei C., Jing X., A comprehensive review on vibration energy harvesting: Modelling and realization, Renewable and Sustainable Energy Reviews vol. 74, 1–18, Pergamon; (2017), DOI: 10.1016/J.RSER.2017.01.073.

[21] Ahmad I., Meng Hee L., M. Abdelrhman A., Asad Imam S., Leong MS., Hybrid vibro-acoustic energy harvesting using electromagnetic transduction for autonomous condition monitoring system, Energy Conversion and Management vol. 258, 115443, Pergamon; (2022), DOI: 10.1016/J.ENCONMAN.2022.115443.

[22] Blokhina E., Aroudi A El., Alarcon E., Galayko D., Nonlinearity in Energy Harvesting Systems: Micro- and Nanoscale Applications, Nonlinearity in Energy Harvesting Systems: Micro- and Nanoscale Applications 1–359, Springer International Publishing; (2016), DOI: 10.1007/978-3-319-20355-3.

[23] Kulik M., Gabor R., Jagieła M., Surrogate Model for Design Uncertainty Estimation of Nonlinear Electromagnetic Vibration Energy Harvester, Energies vol. 15, no. 22, MDPI; (2022), DOI: 10.3390/EN15228601.

[24] Pelz PF., Groche P., Pfetsch ME., Schaeffner M, editors., Mastering Uncertainty in Mechanical Engineering, Cham: Springer International Publishing; (2021), DOI: 10.1007/978-3-030-78354-9.

[25] Yan J., Liu M., Jeong YG., Kang W., Li L., Zhao Y., et al., Performance enhancements in poly(vinylidene fluoride)-based piezoelectric nanogenerators for efficient energy harvesting, Nano Energy vol. 56, 662–92, Elsevier Ltd; (2019), DOI: 10.1016/J.NANOEN.2018.12.010.

[26] Muscat A., Bhattacharya S., Zhu Y., Electromagnetic Vibrational Energy Harvesters: A Review, Sensors (Basel, Switzerland) vol. 22, no. 15, 5555, MDPI; (2022), DOI: 10.3390/S22155555.

[27] Brusa E., Carrera A., Delprete C., A Review of Piezoelectric Energy Harvesting: Materials, Design, and Readout

Circuits, Actuators 2023, Vol. 12, Page 457 vol. 12, no. 12, 457, Multidisciplinary Digital Publishing Institute; (2023), DOI: 10.3390/ACT12120457.

[28] M Ferreira AJ., MATLAB Codes for Finite Element Analysis: Solids and Structures (Solid Mechanics and Its Applications), n.d.,.

[29] Akoun G., Yonnet JP., 3D analytical calculation of the forces exerted between two cuboidal magnets, IEEE Transactions on Magnetics vol. 20, no. 5, 1962–4, (1984), DOI: 10.1109/TMAG.1984.1063554.

[30] Gabor R., Kulik M., Minimalizacja naprężeń elementu sprężystego w nieliniowym przetworniku energii drgań na energię elektryczną, PRZEGLĄD ELEKTROTECHNICZNY vol. 101, no. 6, 76–80, (2025), DOI: 10.15199/48.2025.06.13.

[31] Ferdous W., Manalo A., Peauril J., Salih C., Raghava Reddy K., Yu P., et al., Testing and modelling the fatigue behaviour of GFRP composites – Effect of stress level, stress concentration and frequency, Engineering Science and Technology, an International Journal vol. 23, no. 5, 1223–32, Elsevier; (2020), DOI: 10.1016/J.JESTCH.2020.01.001.

[32] Frascio M., Avalle M., Monti M., Fatigue strength of plastics components made in additive manufacturing: First experimental results, Procedia Structural Integrity vol. 12, 32–43, Elsevier B.V.; (2018), DOI: 10.1016/J.PROSTR.2018.11.109.

[33] Abdurrahman W., Fitri M., The Fatigue Strength Analysis of ABS (Acrylonitrile Butadiene Styrene) Material Shaft Result of 3D Printing Process Due to Rotating Bending Load, Materials Science Forum vol. 1051 MSF, 137–44, Trans Tech Publications Ltd; (2022), DOI: 10.4028/WWW.SCIENTIFIC.NET/MSF.1051.137.

[34] ASM Material Data Sheet, n.d., https://asm.matweb.com/search/SpecificMaterial.asp?bassnum=MA6061T6 (accessed July 8, 2025).

[35] Hirukawa H., Furuya Y., Nishikawa H., Nagashima N., Takeuchi E., NIMS fatigue data sheet on gigacycle fatigue properties of A6061-T6 (Al-1.0Mg-0.6Si) aluminium alloy at high stress ratios, Science and Technology of Advanced Materials: Methods vol. 2, no. 1, 232–49, Taylor & Francis; (2022), DOI: 10.1080/27660400.2022.2085020.

[36] Michel SA., Kieselbach R., Martens HJ., Fatigue strength of carbon fibre composites up to the gigacycle regime (gigacycle-composites), International Journal of Fatigue vol. 28, no. 3, 261–70, (2006), DOI: 10.1016/J.IJFATIGUE.2005.05.005.